

# Analysis of a Critical Residue Determining Herbicide Efficiency Sensitivity in Carboxyltransferase Domain of Acetyl-CoA Carboxylase from Poaceae by Homology Modeling and Free Energy Simulation

TAO Jin, ZHAO Bo, TIAN Xue-mei, ZHENG Liang-yu\* and CAO Shu-gui\*

Key Laboratory for Molecular Enzymology and Engineering of Ministry of Education,  
Jilin University, Changchun 130021, P. R. China

**Abstract** Carboxyltransferase domain(CT) of acetyl-coenzyme A carboxylase(ACCCase, EC 6.4.1.2) from a family of Poaceae is an important target of commercial herbicide APPs for controlling grass weed growth. As the abuse of APPs herbicides, the resistant ACCCase due to the mutation of a single residue(Ile→Leu), which is located in CT active site, is emergent in many populations and species of Poaceae. So it is urgent to understand the resistant mechanism so as to design new effect herbicides. Herein lies the complex of CT dimmer from *Lolium rigidum* and herbicide haloxyfop successfully constructed for wild type enzyme and Ile/Leu mutant, respectively, providing a basis for explaining the resistance from microscopic structure. Moreover, the binding free energy difference between wild type and mutant enzymes was predicted in good agreement with the known observation, and the various contributions to it were analyzed, by Molecular mechanics-Poisson-Boltzmann surface area(MM-PBSA) method. The results indicate the van der Waals interaction difference between the protein and inhibitor,  $-22.94$  kJ/mol of CT wild type lower than that of mutant, is the major reason for resistance. Structure analysis further suggests that van der Waals interaction difference is originated from the steric hindrance between the side chain of mutated residue Leu and the chiral methyl group of haloxyfop. All these findings enhance the understanding of resistant mechanism of ACCCase to herbicide by Ile/Leu mutation and provide an important clue for the rational design of high effective herbicides.

**Keywords** Molecular modeling; Molecular dynamics; Free energy calculation; Herbicide resistance

**Article ID** 1005-9040(2010)-05-816-06

## 1 Introduction

For plants, the chloroplastic acetyl-coenzyme A carboxylase(ACCCase, EC 6.4.1.2), which catalyzes the carboxylation of acetyl-coenzyme A to produce malonyl-coenzyme A, is a committed enzyme in fatty acid biosynthesis<sup>[1-4]</sup>. Two isoformers of chloroplast ACCCase have been identified so far. In the family of Poaceae(grasses), chloroplast ACCCase is a large multidomain enzyme containing the biotin carboxylase (BC) domain, the biotin carboxyl carrier protein (BCCP) domain, and the carboxyltransferase(CT) domain, while in other families of plants, it is a multisubunit enzyme composed of subunits of BC, BCCP, and two subunits for the CT.

Aryloxyphenoxypropionates(APPs) are an important class of commercial green herbicides<sup>[5-8]</sup>. They selectively inhibit chloroplastic ACCCase from

grass by targeting the active site in CT domain, not affecting the ones from other plants. Thus, APPs are widely used in farms and crops field to control grass weeds<sup>[9-12]</sup>. However, as the abuse of these herbicides, more and more APPs-resistant ACCCase mutants have emerged in grass around the world and in many species of family grass<sup>[5,13]</sup>. Extensive researches have found that the resistance of most mutants to herbicides is caused by single residue mutation, and all those mutations occur in the CT domain<sup>[13-23]</sup>. Particularly, an Ile/Leu mutation at the equivalent position is frequently reported in many species of grass, such as *Avena fatua* L. and *Avena sterilis* ssp. *ludoviciana* Durieu(wild oat)<sup>[20]</sup>, *Lolium rigidum* Gaudin(rigid ryegrass)<sup>[17-18]</sup>, *Alopecurus myosuroides* Hudson (black grass)<sup>[14-16]</sup> and *Setaria viridis* L. Beauv (green foxtail)<sup>[19]</sup>. Therefore, it is critically important

\*Corresponding author. E-mail: caosg@jlu.edu.cn; lyzheng@jlu.edu.cn

Received December 3, 2009; accepted January 30, 2010.

Supported by the National Natural Science Foundation of China(Nos.20802025, 30870539, 20432010 and 20672045).

to understand the molecular basis of this resistance caused by Ile/Leu mutation for designing new resistance-evading herbicides. Nevertheless, the experimental techniques are limited to this problem, since the molecular clone of active CT domain from grass is hard<sup>[24]</sup> and their experimental (crystal or NMR) structures have still been unclear until now.

Herein lies the complex of *Lolium rigidum* CT dimer, containing one active site, and herbicide haloxyfop successfully constructed for wild type enzyme and Ile/Leu mutant, respectively, by homology modeling based on the known CT dimer structures from yeast<sup>[25,26]</sup>, providing a basis for explaining the resistance from microscopic structure. Moreover, the relative binding free energy difference between wild type and mutant enzymes was predicted, and various contributions to it were analyzed. By combination of energetic and structural analyses, the possible reasons for the resistance due to Ile/Leu mutation were discussed. As far as we know, it is the first time to explain the ACCase resistant mutation from energetic perspective through MM-PBSA method. All the study may enhance the understanding of ACCase resistance of grass caused by Ile/Leu mutation APPs and provide an important clue for rational design of new high effective herbicides.

## 2 Materials and Methods

### 2.1 Homology Modeling

The structures of truncated haloxyfop/CT-wild-type enzyme and haloxyfop/CT-mutant complexes were homology modeled respectively by using two templates. The target sequence of *Lolium rigidum* was obtained from NCBI (entry AAY27403.1). The crystal structure of the complex of yeast ACCase CT with haloxyfop (PDB entry: 1UYS) was used as the primary template, and the crystal structure of free yeast ACCase CT (PDB entry: 1OD2) was used as the second template to complement missed residues in 1UYS. Sequence alignment was conducted *via* the CLUSTAL X 1.83 program<sup>[27]</sup>, and default parameters were applied. Manual inspection was carried out to further ensure the accuracy of alignment. Following alignment, 10 modeled structures of complex were generated *via* the MODELLER 9v1 program<sup>[28]</sup> with default parameters. The best one was picked out according to the energy function score in MODELLER and then submitted to PROCHECK<sup>[29]</sup> to further evaluate the

quality of modeling.

### 2.2 Molecular Dynamics

The wild-type and mutant complex systems were submitted respectively to molecular dynamics simulation of 2 ns on a cluster of 24 intel Xeron 2 CPU (2.0 GHz) with Amber 9<sup>[30]</sup>. The Cornell force field and GAFF force field were adopted for CT and haloxyfop, separately. Charges of haloxyfop were derived by AM1-BCC method<sup>[31]</sup>.

Considering the complexity of the complexes, elaborate protocols were applied before starting the formal molecular dynamic. First, the modeled haloxyfop-CT complexes were carefully added hydrogen on the titratable residues having multiple protonation states. Then the systems were subjected to energy minimization with decreasing constraint force on the non-hydrogen atoms, *via* generalized Born implicit water model, till the system converged. Next the systems were neutralized by adding Na<sup>+</sup> and solvated in an octahedral box of TIP3P model water, which extended at 1.5 nm from any given atom in the systems. The water enclosed in the system was energy minimized with decreasing constraint force on the protein by a combination of steepest descent method and conjugate gradient method, followed by a minimization with the entire system relaxation.

After the preparing procedures finished, the systems were slowly heated from 0 to 300 K with decreasing force on protein over 100 ps under NVT condition and then run for equilibration and sampled under NPT condition. During the simulation, periodic boundary conditions were accepted. The Particle Mesh Ewald method<sup>[32]</sup> was selected for periodic long range electrostatic interaction and a 1.0 nm cutoff for nonbonding van der Waals interactions. All the bonds involving hydrogen atoms were constrained with the SHAKE algorithm<sup>[33]</sup>. Constant temperature 300 K was maintained *via* the Langevin dynamics with a collision frequency of 1.0. Constant pressure  $1.013 \times 10^5$  Pa was controlled by isotropic position scaling with a pressure relaxation time of 2.0 ps. A time step of 2 fs was used to integrate the equations of motion. The coordinates were saved every 2 ps during the entire simulation process.

### 2.3 Binding Free Energy Calculation

MM-PBSA method<sup>[34]</sup> was used to estimate

binding affinity and selectivity with AMBER 9. By this method, the total free energy of a system( $G$ ) was evaluated as a sum of the MM gas-phase energy( $E_{MM}$ ), solvation free energy( $G_{sol}$ ), and entropy contribution( $-TS$ ).

$$G = G_{sol} + E_{MM} - TS \quad (1)$$

$$E_{MM} = E_{ele} + E_{vdw} \quad (2)$$

$$G_{solv} = G_{pb} + G_{np} \quad (3)$$

$$G_{np} = \gamma SASA + \beta \quad (4)$$

Then the binding free energy was estimated by Eq.(5) for a given complex system.

$$\Delta G_{bind} = G_{complex} - (G_{protein} + G_{ligand}) \quad (5)$$

The MM gas-phase energy including electrostatic energy( $E_{ele}$ ) and van der Waals interaction( $E_{vdw}$ ) was directly calculated by Sander with non-cutoff. Electrostatic solvation free energy( $G_{pb}$ ) can be well calculated by the solution to the PB equation, with dielectric constant 1 for the solute and constant 80 for the solvent water. The nonpolar solvation energy( $G_{np}$ ) was obtained by means of equation (4) with parameters  $\gamma = 0.0227$  kJ/mol and  $\beta = 3.85$  kJ/mol, in which the solvent-accessible-surface area(SASA) was estimated by Morsulf. Note that entropy contribution term was neglected here, since our aim was to calculate the relative binding free energy difference and the entropy contribution to the structure-similar inhibitor was

already known to be almost the same.

150 structures were sampled from the MD trajectory from 500 ps to 2000 ps for both haloxyfop/CT-wild-type enzyme and haloxyfop/CT-mutant complexes at 10 ps intervals. The final averages of binding free energy over these samples were taken to compute the binding energy difference between CT wild type enzyme and mutant.

### 3 Results and Discussion

#### 3.1 Homology Modeling

Homology modeling of proteins is currently the most accurate method for the prediction of 3D structure, yielding models suitable for a wide spectrum of application, such as investigations into mechanism, structure-based drug development, and virtual screening<sup>[35–38]</sup>. This approach can produce a reasonable structural model for any given protein sequence that has relative template having more than 25% amino acid sequence identity<sup>[39]</sup>. Our alignment shows that the *Lolium rigidum* and yeast CT dimmers share a high sequence identity of 59%(Fig.1), indicating that the homology modeling is practicable for our target.

The best inhibitor-protein complex model, having the lowest energy score based on the Modeller energy

```

Yeast_N      EYPRGRQFVVVANDITFKIGSFGPQDEDFNFKVTEYARKKGIPIIYLAANSGARIGMAEE
Lolium_N     EFPSCRQIIVVANDITFRAGSFGFRDAPFEAVTNLACBRKPLIYLAANSGARIGIADE
          :* * * * : * * * * * * * * * * * * * * * * * * * * * * * * * * * * * *
Yeast_N      IVPLFQVAWINDAANFDKGFQYL YLTSBGMETLKKPKDKNSVLTERTVIN-GEERFVIKTI
Lolium_N     VKSIFRVKWIIDSNPERGFDVYVLS-E--EDYGRISS--SVLAHKQLDSCGIRWVIDSV
          : . : * * * * * : * * * * * * * * * * * * * * * * * * * * * * * *
Yeast_N      IGS EDGLGVBC L RGSGLIAGATSRAYHDIFITITLVTORSVGIGAYLVRLOQRAIQVEGQP
Lolium_N     VKE EDGLGVEN I HGSAAIASAYSRAYEBTFITLFPVTGRVIGIGAYLARLGRICIQREDQP
          : * . * * * * * * * * * * * * * * * * * * * * * * * * * * * * * *
Yeast_N      IILTGAPAINKMLG
Lolium_N     IILTGYSALNKLLG
          * * * * * . * : * * * * *
Yeast_C      GIPLGVIGVETRIVENLIPADPANFNSAETL IQEPQGVHWFNSAFKTAQAINDFNNGEQL
Lolium_C     GIPLGVIGVETRIVENLIPADPANFNSAETL IQEPQGVHWFNSAFKTAQAMLDPNR-EGL
          * * * * * * * * * * * * * * * * * * * * * * * * * * * * * *
Yeast_C      PMMILANWRGFSGQQRDMFNEVLKYGSFIVDALVDYKQP I IYIPPTGELRGGSWVVVDP
Lolium_C     PLF ILANWRGFSGQQRDLFXGILQAGSTIVENLRXYNQPAFVYIPKAAELRGGAWVIDS
          * : * * * * * * * * * * * * * * * * * * * * * * * * * * * * *
Yeast_C      TINADQMEMYADVNRAGVLEPQGMVGIKPRREKLLDTMNRLLDDKYRELRSQLS--NKS
Lolium_C     KINPDRIBCYAETTAKGNVLEPQGLIEIKPRSEELQECMGRLDPELINLKAQLGQAKHEN
          . * * : * * * * * * * * * * * * * * * * * * * * * * * * * *
Yeast_C      LAPEVHQQISKQLADRRELLPIYQGIS
Lolium_C     GSLSDGBSIQKSIBARKQLLPLYQTIA
          : . : . * * * * * : * * * * * * * * *

```

Fig.1 Sequence alignment of yeast and *Lolium rigidum* CT dimmers

This active site-containing CT dimer consists of the N subdomain of one monomer(indicated with suffix 'N') and the C subdomain of the other monomer(indicated with suffix 'C'). The residues are marked with asterisk(\*), colon(:) and dot(.) based on decreasing similarity, and the least similar residues are not marked. The mutated residual position is indicated with bigger size letter.

function, was selected from the 10 models for both wild-type enzyme and mutant, separately. The Procheck examination shows the 91.2% or 90.0% residues (without glycine and proline) of CT dimmer are located in the most favoured regions for wild type or mutant enzyme, consistent with the expectation of having over 90% in the most favoured regions (Fig.2). In particular, all active site residues are located in the most favoured regions, while the residues in the other regions are almost positioned at random coil and/or the surface of protein. All these findings suggest the constructed models are reasonable, and suitable for the following thermodynamic study.

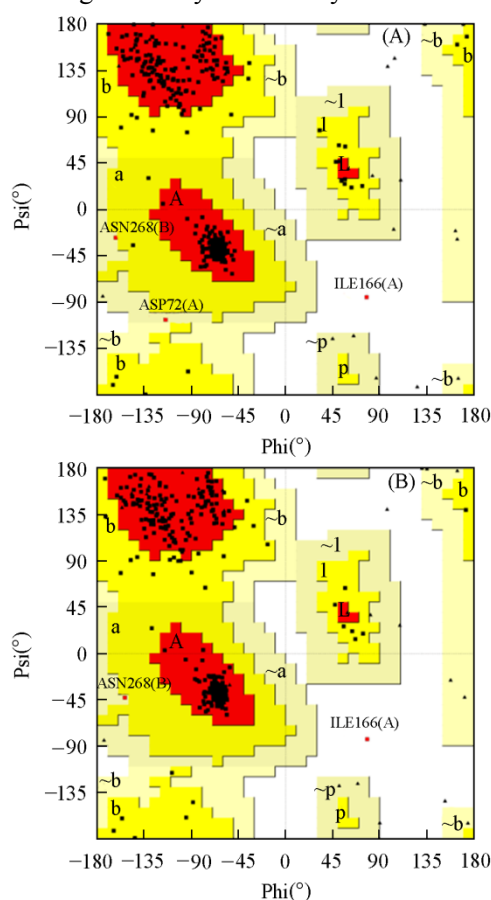


**Fig.2 Ramachandran plots of wild(A) and mutant(B) CT**

These plots were produced by Procheck. In the wild CT, 91.2%, 7.9%, 0.6% and 0.3% residues are in most favoured regions [A, B, L], additional allowed regions [a, b, l, p], generously allowed regions [ca. a, ca. b, ca. l, ca. p] and disallowed regions, respectively. In the mutant CT, 90.0%, 9.4%, 0.3% and 0.3% residues are in most favoured regions [A, B, L], additional allowed regions [a, b, l, p], generously allowed regions [ca. a, ca. b, ca. l, ca. p] and disallowed regions.

### 3.2 Molecular Dynamics and Binding Free Energy

In order to obtain ample dynamics information for free energy calculation, both the systems, haloxyfop/CT-wild-type and haloxyfop/CT-mutant

complexes, were run for a simulation of 2.0 ns. The root mean square deviation (RMSD) values of *alpha* carbon from their starting structures were calculated, respectively (Fig.3).

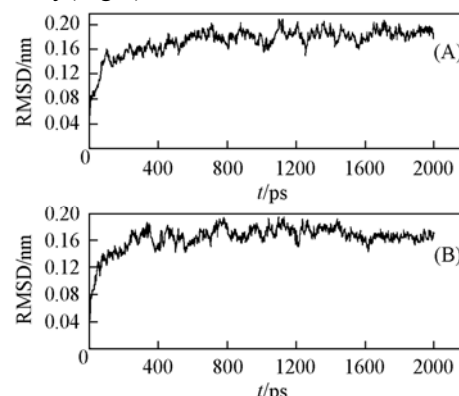


**Fig.3 Root mean square derivation (RMSD) from starting structure along time**

(A) Wild type CT; (B) CT mutant.

For both the wild type and mutant, the RMSD increases quickly during the first 300 ps and then reaches a plateau, indicating the system is thermodynamic equilibration. In this context, the conformation information was sampled for binding free energy calculation from 500 ps to 2000 ps at intervals of 10 ps. The average structure of the 150 sampled structures was constructed for the following structure analysis.

The MM-PBSA method we used is a reliable and popular approach in binding free energy calculation and has been successfully used for reproducing or predicting the experimental results for many systems<sup>[34,40–44]</sup>. Table 1 presents the binding free energy components of both CT wild type and mutant, and their difference, calculated by MM-PBSA.

**Table 1 Binding free energy components for both CT wild type and mutant complexes<sup>a</sup>**

Energy	Wild-type	Mutant	$\Delta^b$
$\langle \Delta E_{\text{ele}} \rangle$	$-8.25 \pm 5.15$	$-9.13 \pm 5.61$	0.88
$\langle \Delta E_{\text{vdw}} \rangle$	$-201.55 \pm 10.55$	$-178.61 \pm 11.68$	$-22.94$
$\langle \Delta E_{\text{MM}} \rangle$	$-209.80 \pm 10.51$	$-187.74 \pm 10.89$	$-22.06$
$\langle \Delta G_{\text{np}} \rangle$	$-20.26 \pm 0.50$	$-19.18 \pm 0.34$	$-1.09$
$\langle \Delta G_{\text{pb}} \rangle$	$27.30 \pm 10.93$	$28.93 \pm 11.47$	$-1.63$
$\langle \Delta G_{\text{sol}} \rangle$	$7.03 \pm 11.17$	$9.76 \pm 11.76$	$-2.72$
$\langle \Delta G_{\text{tot}}^{\text{ele}} \rangle^c$	$19.05 \pm 6.82$	$19.80 \pm 7.62$	$-0.75$
$\langle \Delta G_{\text{tot}} \rangle$	$-202.77 \pm 10.80$	$-177.98 \pm 11.34$	$-24.79$

<sup>a</sup> Entropy term is not included in the binding free energy and all the values in the table are given in kJ/mol; <sup>b</sup> the difference is calculated by Component(wild-type) - Component(mutant); <sup>c</sup>  $\langle \Delta G_{\text{tot}}^{\text{ele}} \rangle = \langle \Delta E_{\text{ele}} \rangle + \langle \Delta G_{\text{pb}} \rangle$ .

The result shows the total binding free energy of wild type is  $-24.79$  kJ/mol lower than that of mutant, suggesting the haloxyfop-binding affinity of wild type CT is 2 orders of magnitude as strong as that of mutant CT. This finding is in good agreement with the real observation that the wild type CT is sensitive to

haloxyfop, while the mutant encounters resistance with this herbicide. Further free energy decomposition analysis indicates the binding free energy difference is majorly caused by the difference between the van der Waals interactions ( $\Delta E_{vdw}$ ),  $-22.94$  kJ/mol (Table 1); while the difference between the solvation free energies ( $\Delta G_{sol}$ ) or Coulomb interactions ( $\Delta E_{ele}$ ) has tiny effect on the total binding energy difference. In other words, the van der Waals interaction difference is shown to be the major reason for the mutant resistance.

The reason for mutant resistance is thus clearly indicated from the thermodynamics energetic perspective. Besides it, the structure analysis was also carried out, which provides more microscopic and intuitional insight. Fig.4 shows the binding of haloxyfop to active site of wild type(or mutant) CT, where the surface of CT is constructed and colored according to the electrostatic potential.

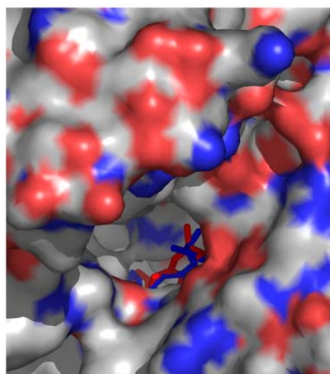


**Fig.4** Haloxyfop binding into the active site of CT dimer

The surface of CT dimer is constructed and colored according to electrostatic potential. The red color presents the positive potential. The blue presents the negative potential, and the white presents the values near zero (hydrophobic). The location of haloxyfop is indicated by stick model for wild type CT and mutant, respectively. The haloxyfop in wild type CT is indicated by red, and the one in mutant is indicated by blue.

From Fig.4, it is clearly shown that the binding site is a hydrophobic or non polar cavity although the surface of CT is hydrophilic or polar. Considering the binding site is hydrophobic, it can thus be inferred that solvation free energy ( $\Delta G_{sol}$ ) or Coulomb interaction ( $\Delta E_{ele}$ ) is small in the total binding energy and has a little effect on the total binding free energy difference. This structural finding is in good agreement with the previous energetic findings. Notably, it has also been observed that the side chain of mutated Leu residue in mutant conflicts a little with the methyl group of haloxyfop, while this steric hindrance does not exist in the corresponding Ile in wild-type CT(Fig.5).

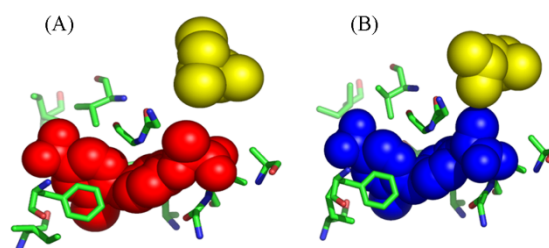


**Fig.5** Binding mode of haloxyfop with wild type CT dimer(A) or mutant(B)

The residues in active site are presented by sticks. The haloxyfop and critical residue, Ile or Leu, are presented by ball with van der Waals radius.

Obviously, the presence and absence of steric hindrance can result in the large van der Waals interaction difference. So, it is reasonable to propose that the previous calculated van der Waals interaction difference is the result of steric hindrance caused by Ile/Leu mutation, and this steric hindrance caused by Ile/Leu mutation results in the change of ACCase from sensitive to resistant.

## 4 Conclusions

In this article, the complexes of ACCase CT dimer and haloxyfop were successfully constructed for both sensitive wild type and resistant mutant *Loium rigidum*. Their relative binding free energy was also predicted by MM-PBSA method, well consistent with the real observation. The free energy components analysis indicates the van der Waals interaction difference is the major reason for the resistance. Structural study further shows that this van der Waals interaction difference originated from the steric hindrance between the critical mutated residue Leu and haloxyfop, not found between the wild Ile and haloxyfop. All these findings may give an enhanced understanding of inhibition mechanism of ACCase and provide an important clue for rational design of high effective herbicides.

## Acknowledgment

The authors acknowledge the Professor Feng Yan for the usage of software Amber9.

## References

- [1] Wakil S. J., Stoops J. K., Joshi V. C., *Ann. Rev. Biochem.*, **1983**, 52, 537
- [2] Nikolau B. J., Ohlrogge J. B., Wurtele E. S., *Arch. Biochem. Biophys.*, **2003**, 414, 211
- [3] Harwood J. L., *Annu. Rev. Plant. Physiol.*, **1988**, 39, 101
- [4] Sasaki Y., Nagano Y., *Biosci. Biotechnol. Biochem.*, **2004**, 68, 1175
- [5] Devine M. D., Shukla A., *Crop. Prot.*, **2000**, 19, 881

- [6] Golz A., Focke M., Lichtenthaler H. K., *J. Plant Physiol.*, **1994**, 143, 426
- [7] Holt J. S., Powles S. B., Holtum J. A. M., *Annu. Rev. Plant Physiol. Plant Mol. Biol.*, **1993**, 44, 203
- [8] Konishi T., Sasaki Y., *Proc. Natl. Acad. Sci.*, **1994**, 91, 3598
- [9] Alban C., Baldet P., Douce R., *Biochem. J.*, **1994**, 300, 557
- [10] Egli M. A., Gegenbach B. G., Gronwald J. W., Somers D. A., Wyse D. L., *Plant Physiol.*, **1993**, 101, 499
- [11] Burton J. D., Gronwald J. W., Keith R. A., Somers D. A., Gegenbach B. G., Wyse D. L., *Pestic. Biochem. Physiol.*, **1991**, 39, 100
- [12] Rendina A. R., Craig-Kennard A. C., Beaudoi J. D., KBreen M. J., *J. Agric. Food Chem.*, **1990**, 38, 1282
- [13] Liu W., Harrison D. K., Chalupska D., Gornicki P., O'Donnell C. C., Adkins S. W., Haselkorn R., Williams R. R., *Proc. Natl. Acad. Sci.*, **2007**, 104, 3627
- [14] Brown A. C., Moss S. R., Wilson Z. A., Field L. M., *Pestic. Biochem. Physiol.*, **2002**, 72, 160
- [15] Delye C., Calmes E., Matejcek A., *Theor. Appl. Genet.* **2002**, 104, 1114
- [16] Delye C., Matejcek A., Gasquez J., *Pest. Manag. Sci.*, **2002**, 58, 474
- [17] Zagnitko O., Jelenska J., Tevzadze G., Haselkorn R., Gornicki P., *Proc. Natl. Acad. Sci. USA*, **2001**, 98, 6617
- [18] Zhang X. Q., Powles S. B., *Planta*, **2006** 223, 550
- [19] Delye C., Wang T. Y., Darmency H., *Planta*, **2002**, 214, 421
- [20] Christoffers M. J., Berg M. L., Messersmith C. G., *Genome*, **2002**, 45, 1049
- [21] White G. M., Moss S. R., Karp A., *Weed Res.*, 2005, 45, 440
- [22] Delye C., Zhang X. Q., Chalopin C., Michel S., Powles S. B., *Plant Physiol.*, **2003**, 132, 1716
- [23] Delye C., Zhang X. Q., Michel S., Matejcek A., Powles S. B., *Plant Physiol.*, **2005**, 137, 794
- [24] Yang X. Y., Tao J., Zheng L. Y., Wang R. J., Zhao K., Cao S. G., *Chem. Res. Chinese Universities*, **2009**, 25(5), 690
- [25] Zhang H., Yang, Z., Shen, Y., Tong, L., *Science*, **2003**, 299, 2064
- [26] Zhang H., Tweel B., Tong L., *Proc. Natl. Acad. Sci. USA*, **2004**, 101, 5910
- [27] Thompson J. D., Gibson T. J., Plewniak F., Jeanmougin F., Higgins D. G., *Nucleic. Acids Res.*, **1997**, 25, 4876
- [28] Marti-Renom M. A., Stuart A., Fiser A., Melo F., Sali A., *Annu. Rev. Biophys. Biomol. Struct.*, **2000**, 29, 291
- [29] Laskowski R. A., MacArthur M. W., Moss D. S., Thornton J. M., *J. Appl. Cryst.*, **1993**, 26, 283
- [30] Case D. A., Darden T. A., Cheatham T. E., Darden T., Paesani F., *Amber 9*, University of California, San Francisco, **2006**
- [31] Jakalian A., Bush B. L., Jack D. B., Bayly C. I., *J. Comput. Chem.*, **2000**, 21, 132
- [32] Essmann U., Perera L., Berkowitz M. L., Darden T., Lee H., Pedersen L. G., *J. Chem. Phys.*, **1995**, 103, 8577
- [33] Ryckaert J. P., Ciccotti G., Berendsen H. C. J., *J. Comput. Phys.*, **1977**, 23, 327
- [34] Kollman P. A., Massova I., Reyes C., Kuhn B., Huo S., Chong L., Lee M., Lee T., Duan Y., Wang W., Donini O., Cieplak P., Srinivasan J., Case D. A., Cheatham T. E., *Acc. Chem. Res.*, **2000**, 33, 889
- [35] Li M., Wang B., *J. Mol. Model.* **2007**, 13, 1237
- [36] Du L. P., Li M. Y., Tsai K. C., You Q. D., Xia L., *Biochem. Biophys. Res. Commun.*, **2005**, 332, 677
- [37] Ginalski K., *Curr. Opin. Struct. Biol.*, **2006**, 16, 172
- [38] Du L., Li M., You Q., Xia L., *Biochem. Biophys. Res. Commun.*, **2007**, 355, 889
- [39] Tramontano A., *Methods*, **1998**, 14, 293
- [40] Wang J., Morin P., Wang W., Kollman P. A., *J. Am. Chem. Soc.*, **2001**, 123, 5221
- [41] Wang W., Kollman P. A., *Proc. Natl. Acad. Sci.*, **2001**, 98, 14937
- [42] Kuhn B., Kollman P. A., *J. Am. Chem. Soc.*, **2000**, 122, 3909
- [43] Zoete V., Meuwly M., Karplus M., *Proteins*, **2005**, 61, 79
- [44] Kuhn B., Kollman P. A., *J. Med. Chem.*, **2000**, 43, 3786